

Harmonic generation in CO₂ laser target interaction

N. H. Burnett, H. A. Baldis, M. C. Richardson, and G. D. Enright

National Research Council of Canada, Division of Physics, Ottawa, K1A 0R6, Canada
(Received 23 March 1977; accepted for publication 17 May 1977)

We report the observation of an extended series of integral harmonic lines in the spectrum of direct backscatter of 10.6- μm radiation incident at intensities $> 10^{14} \text{ W/cm}^2$ onto planar solid targets. We have observed and spectrally resolved up to the eleventh harmonic (0.95 μm) at intensities well above the plasma continuum background.

PACS numbers: 52.25.Ps, 52.50.Jm, 52.40.Db, 42.65.Cq

Second harmonic generation in laser-solid interaction has been the object of considerable theoretical¹⁻³ and experimental⁴⁻⁷ interest in recent years. Subharmonic generation in the underdense corona of the interaction has also been studied and applied as a diagnostic.⁸ Experiments using short-pulse CO₂ laser radiation (10.6 μm) have been distinguished from 1.06- μm experiments by a much lower level of backscattered $\frac{3}{2}\omega_0$ emission⁹ and the observation in the 10.6- μm studies of an additional harmonic line at $\omega = 3\omega_0$,⁹ a possibility which existing theories on harmonic generation seem to have largely overlooked.

We wish to report the existence of a complete series of integral harmonic lines at reasonably high intensity extending from the third up to at least the eleventh harmonic in the backscatter from plasmas produced by focusing a nanosecond 10.59- μm pulse from the COCO-II¹⁰ laser at NRC onto solid Al targets in vacuum.

For the purposes of these studies, the laser was operated on a single rotational line (P20) in the 10.4- μm vibrational band, producing pulses with energy in the range 20–50 J, depending on the number of amplifiers utilized, and a duration of 1.8–2.0 ns (FWHM) in a nearly diffraction-limited 8-cm-diam beam. Prepulse energy was carefully monitored and for the measurements reported here did not exceed a few hundred microjoules. A 20-cm focal length off-axis parabolic mirror was used to focus the beam to a $\sim 150\text{-}\mu\text{m}$ -diam spot, limited by the optical quality of the mirror, on the surface of flat Al targets, as shown in Fig. 1. The laser beam was polarized with its **E** vector in the plane of incidence and the target normal was $\sim 20^\circ$ from the direction of the incident beam.

A portion of the collimated backscatter was sampled with a beamsplitter $\sim 3 \text{ m}$ upstream from the target

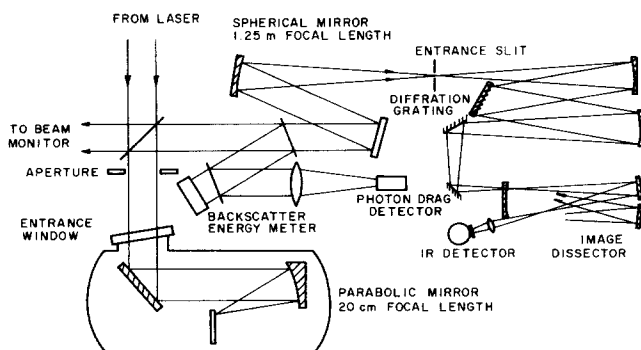


FIG. 1. Schematic of experimental arrangement.

and the target focal spot was imaged with $6\times$ magnification onto crossed 500- μm slits at the entrance to a 2-m grating spectrograph. The backscattered spectrum was analyzed with a passive image dissector at the spectrograph output.¹¹ This device focused ~ 25 channels of spectral information onto a single detector with a time delay of 13 ns between channels. Thus the fundamental and harmonic lines in the backscattered light could be spectrally resolved on a single-shot basis.

For incident laser energy in the range 20–50 J, backscattered radiation at the fundamental (10.59 μm) was observed to account for 4–6% of the incident energy. Its spectrum typically peaked near the incident wavelength and exhibited a red wing extending several hundred angstroms within which a periodic spectral structure was often apparent. Harmonics of the fundamental have been observed at $2\omega_0$, $3\omega_0$, $4\omega_0$, $5\omega_0$, and $6\omega_0$ using a high-speed Hg:Cd:Te detector (rise time 1 ns) and at $10\omega_0$ and $11\omega_0$ using a (S1) photomultiplier (rise time 1.4 ns). Observations at $7\omega_0$, $8\omega_0$, and $9\omega_0$ were precluded by the lack of a suitable detector. The identified harmonic lines and their energy levels relative to the backscattered fundamental are summarized in Fig. 2. The bars for the first five harmonics represent shots in the incident energy range 20–50 J, while those for the tenth and eleventh harmonics represent shots in the energy range 40–50 J. Although the individual levels are susceptible to small uncer-

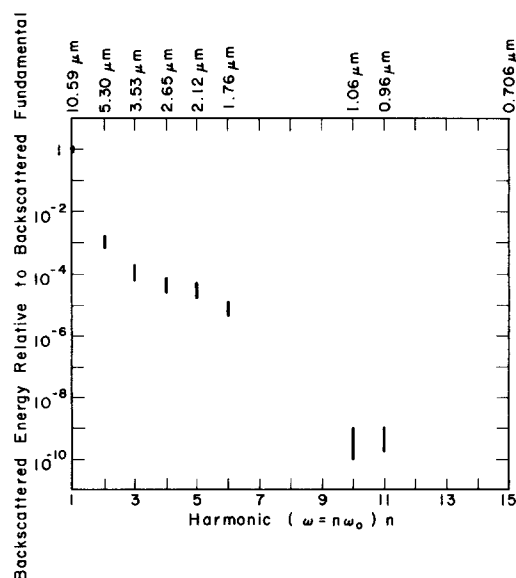


FIG. 2. Levels of integral harmonics observed with incident energy in range 25–50 J.

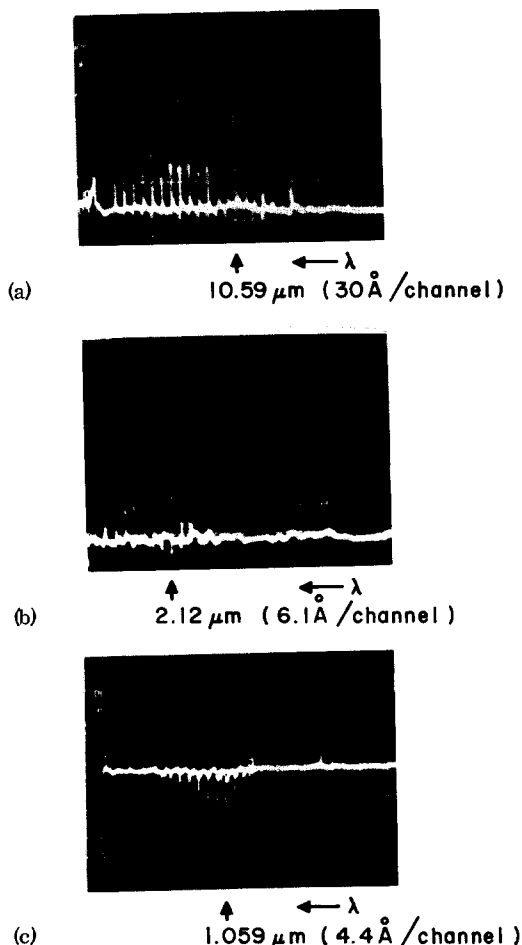


FIG. 3. Dissector output showing backscattered line (a) at fundamental, (b) at $5\omega_0$, (c) at $10\omega_0$. (a) and (b) were recorded using a Hg: Cd: Te detector and (c) using an S1 photomultiplier. The first and last positive pulses in (a) and (c) are timing marks.

tainties in grating transmission and detector spectral response, it can be seen that from the second to eleventh harmonic a decrement between successive harmonic energies $E_j/E_{j+1} \sim 6$ is indicated. A careful search for harmonic lines in the incident laser beam confirmed their absence at limits of detectability that were several orders of magnitude lower than the observed levels in the target backscatter.

Typical raw spectra at ω_0 , $5\omega_0$, and $10\omega_0$ are shown in Fig. 3. These spectra were obtained with the grating tuned to the first, fourth, and ninth orders, respectively, and with the addition of suitable filters in front of the detector to reject unwanted orders. A search was also made for the fifteenth harmonic ($0.706 \mu\text{m}$) using an (S20) photomultiplier but at this wavelength a harmonic line was not observed over the increasing plasma continuum background. Single-shot spectra at ω_0 , $2\omega_0$, $3\omega_0$, $4\omega_0$, $5\omega_0$, and $10\omega_0$ which have been corrected for a slight nonuniformity in the dissector transmission are shown in Fig. 4. The absolute wavelength calibration in these spectra has an uncertainty of ± 0.5 channels. It can be seen that the higher harmonics have a nearly constant spectral width $\delta\lambda/\lambda \sim 2 \times 10^{-3}$ and are significantly skewed to the red.

Although a study of the polarization of the first few harmonics was not possible due to the lack of a suitable polarizer, the eleventh harmonic emission was examined with a Glan polarizer and found to be strongly polarized parallel to the \mathbf{E} vector of the incident laser.

Due to the lack of a suitable interference filter and the high level of $3\omega_0$ harmonic it was not possible to isolate any possible emission at $\frac{3}{2}\omega_0$ in the present experiments. Using glass attenuators however it was possible to set an upper limit on $\frac{3}{2}\omega_0$ emission at about 10^{-5} of backscatter at fundamental or 10^{-1} of the $3\omega_0$ level. This low level of $\frac{3}{2}\omega_0$ emission remains an important distinction between 1.06- and $10.6\text{-}\mu\text{m}$ experiments and is likely indicative of much steeper density gradients near quarter critical in the latter case. It is interesting to note that $\frac{3}{2}\omega_0$ emission has been observed from $10.6\text{-}\mu\text{m}$ solid interaction experiments using longer pulses^{12,13} and from short pulse underdense gas breakdown at $10.6 \mu\text{m}$.¹⁴

The harmonic generation observed here does not appear to fall within the analytical framework of existing theories which concentrate mainly on second harmonic production. It seems likely that the higher harmonics are associated with plasma wave generation through optical resonance which has already been proposed as the source of $2\omega_0$ emission.² In this case coupling to the higher harmonics would improve as the critical density scale length decreases. Although a detailed study of the effect of target orientation on harmonic production remains to be completed it is worth noting that the geometry used here is optimal for optical resonance if the density scale length is $\sim 10 \mu\text{m}$. Thus with an appropriate development of the theory these higher harmonics may prove to be a useful diagnostic in the study of profile modification and resonance absorption in $10\text{-}\mu\text{m}$ interaction experiments. Such an extension of the theory has recently been discussed by Giovanielli and Godwin.¹⁵

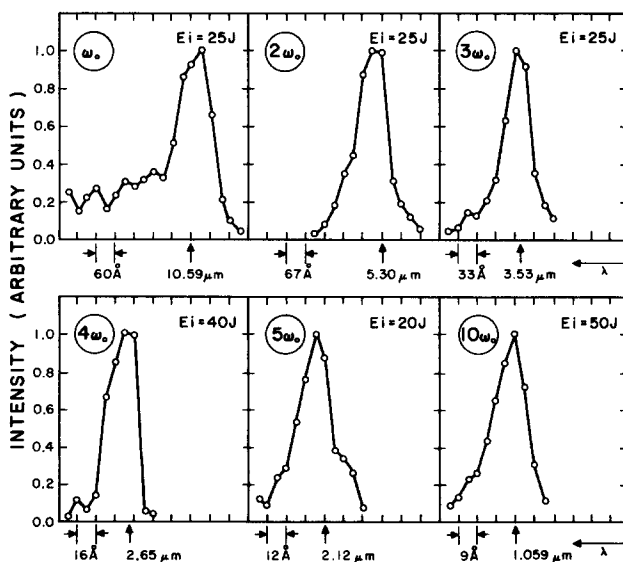


FIG. 4. Typical corrected single-shot spectra at ω_0 , $2\omega_0$, $3\omega_0$, $4\omega_0$, $5\omega_0$, and $10\omega_0$. E_i refers to incident laser energy. The open circles represent individual spectral channels.

The authors would like to acknowledge the continuing technical assistance of G.A. Berry and P. Burtyn.

- ¹J.L. Bobin, M. Decroisset, B. Meyer, and Y. Vitel, *Phys. Rev. Lett.* **30**, 594 (1973).
- ²A.V. Vinogradov and V.V. Pustalov, *Sov. Phys.-JETP* **36**, 492 (1973).
- ³N.S. Erokhin, S.S. Moiseev, and V.V. Mukhin, *Nucl. Fusion* **14**, 333 (1974).
- ⁴Ping Lee, D.V. Giovanielli, R.P. Godwin, and G.H. McCall, *Appl. Phys. Lett.* **24**, 406 (1974).
- ⁵C. Yamanaka, T. Yamanaka, T. Sasaki, J. Mizui, and H.B. Kang, *Phys. Rev. Lett.* **32**, 1038 (1974).
- ⁶H.A. Baldis, H. Pépin, T.W. Johnson, and K.J. Parbhakar, *Phys. Rev. Lett.* **35**, 37 (1975).
- ⁷K. Eidmann and R. Sigel, *Phys. Rev. Lett.* **34**, 799 (1975).

- ⁸Steven Jackel, Bruce Perry, and Moshe Lubin, *Phys. Rev. Lett.* **37**, 95 (1976).
- ⁹H.A. Baldis, H. Pépin, and B. Grek, *Appl. Phys. Lett.* **27**, 292 (1975).
- ¹⁰M.C. Richardson, N.H. Burnett, H.A. Baldis, G.D. Enright, R. Fedosejevs, N.R. Isenor, and I.V. Tomov, *Laser Interaction and Related Plasma Phenomena*, Troy, N.Y., 1976 (unpublished).
- ¹¹H.A. Baldis, N.H. Burnett, and M.C. Richardson, *Rev. Sci. Instrum.* **48**, 173 (1977).
- ¹²E. Fabre, C. Garban, C. Popovics, A. Poquerusse, C. Stena, and J. Virmont, *Proc. 6th Int. Conf. on Plasma Physics and Controlled Nuclear Fusion Research*, Berchtesgaden, 1976 (unpublished).
- ¹³C. Yamabe, E. Setogama, A. Thein, M. Yokogama, and C. Yamanaka, *Jpn. J. Appl. Phys.* **16**, 131 (1977).
- ¹⁴N.H. Burnett, H.A. Baldis, G.D. Enright, M.C. Richardson, and P.B. Corkum, *J. Appl. Phys.* (to be published).
- ¹⁵D.V. Giovanielli and R.P. Godwin, *Am. J. Phys.* **43**, 808 (1975).

Fabrication of long fibers by an improved chemical vapor deposition method (HCVD method)

Takeshi Akamatsu, Koji Okamura, and Yoichi Ueda

Fujitsu Laboratories Limited, Okubo-cho, Akashi, 674 Japan
(Received 7 March 1977; accepted for publication 5 May 1977)

An improved (CVD) method was developed to fabricate long fibers. He gas mixed with O₂ and raw material vapors were introduced into the CVD gas system to increase the deposition rate. This produced a sixfold increase compared to the conventional method. In addition to GeO₂, a small amount of P₂O₅ was added as a dopant to the fused silica to lower the fusion temperature of the deposited soot and minimize tube deformation during the deposition process. Step index fibers 8.5 km long were prepared. These exhibited a mean loss of 4.4 dB/km at a wavelength of 0.85 μm. The outer and the core diameters were 125 and 62.5 μm, respectively.

PACS numbers: 42.80.Lt, 42.80.Mv, 81.15.Gh

The (CVD) method¹ is very useful for fabricating low-loss optical fibers. However, the penalty for this method is a deposition rate that is too low to obtain sufficient thickness of homogeneous glass layers for long fibers. Therefore, this method is disadvantageous for commercial production of fibers. Recently, we have developed a high-deposition-rate CVD method² which uses an addition of He to the gas stream (HCVD method). By this method, we have succeeded in producing low-loss multimode fibers up to 8.5 km.

In the case of the conventional method, a large volume of soot cannot be fused to homogeneous glass without bubbles, because O₂, Cl₂, and Ar adsorbed in the soot remain in the glass layer as bubbles during the

successive fusion process. On the other hand, He gas is presumed to diffuse readily through the glass network structure because of its small atomic radius and it purges other gases during the fusion process. According to our experiments, this assumption was confirmed. Introduction of He was effective in suppressing the generation of bubbles. Therefore, a large volume of soot can be fused to homogeneous glass. Accordingly, this improved method is desirable for preparing large volume preforms with enough thickness of the deposited core glass layer to make long multimode fibers. This

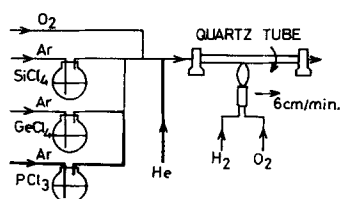


FIG. 1. Schematic diagram of HCVD method.

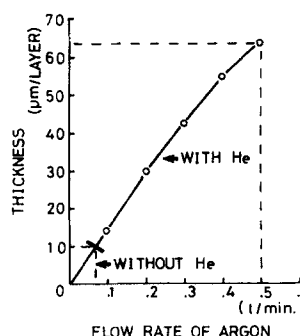


FIG. 2. Flow rate versus thickness of deposited glass layer.